



Article

Piecewise Iterative Extrapolation Method for Bandlimited Signal

Yusi Zhang ^{1,2} , Xuejun Sha ¹, Xiaojie Fang ^{1,2,*} and Xu Lin ¹ 

¹ School of Electronics and Information Engineering, Harbin Institute of Technology, Harbin 150001, China; yszhang@hit.edu.cn (Y.Z.); shaxuejun@hit.edu.cn (X.S.); linxu99@126.com (X.L.)

² Science and Technology on Communication Networks Laboratory, Shijiazhuang 050051, China

* Correspondence: fangxiaojie@hit.edu.cn

Abstract: In some high spectrally efficient communication structures, the Gerchberg-Papoulis extrapolation algorithm can be used to reconstruct nonorthogonal signals. However, the extrapolation efficiency and accuracy degrades when the energy of known signal is small or the iterative filter bandwidth is large. Focused on these drawbacks, a piecewise iterative extrapolation method is proposed to extrapolate bandlimited signals with higher extrapolation efficiency and accuracy. In this paper, the amplitude change of the unknown part over iterations is analyzed and the feasibility of the proposed extrapolation method is discussed. Numerical simulation shows the accuracy superiority of proposed method with the frequency offset compared to the GP algorithm with fixed computational complexity. Besides, the feasibility of the proposed method is verified in fractional Fourier domain with performance advantages.

Keywords: bandlimited signal extrapolation; iteration filter; fractional Fourier transform; Gerchberg-Papoulis algorithm; extrapolation efficiency



Citation: Zhang, Y.; Sha, X.; Fang, X.; Lin, X. Piecewise Iterative Extrapolation Method for Bandlimited Signal. *Electronics* **2022**, *11*, 1175. <https://doi.org/10.3390/electronics11081175>

Academic Editor:
Piotr Zwierzykowski

Received: 15 March 2022

Accepted: 6 April 2022

Published: 7 April 2022

Publisher's Note: MDPI stays neutral with regard to jurisdictional claims in published maps and institutional affiliations.



Copyright: © 2022 by the authors. Licensee MDPI, Basel, Switzerland. This article is an open access article distributed under the terms and conditions of the Creative Commons Attribution (CC BY) license (<https://creativecommons.org/licenses/by/4.0/>).

1. Introduction

The extrapolation for bandlimited signals is one of essential research objects in signal processing, wireless communication, and positioning scenarios where the transmitted signals are always bandlimited. For example, cosine signals and orthogonal frequency division multiplexing (OFDM) signals concentrate its information within a finite bandwidth in the frequency domain, as with the chirp-based signals in the fractional Fourier domain. Due to transmission interference or device failure, only partial data can be detected or used for subsequent processing [1–3]. Besides, the ever-evolving communications scenarios requires improved throughput to satisfy larger access demand, diversity, and mobility [4–8]. Signals are designed to be transmitted partially to obtain higher spectral efficiency according to the high-throughput requirements [8–11]. The reconstruction method in terms of the received partial signals is necessary to maintain the system workability.

The Gerchberg-Papoulis (GP) algorithm, as a classic iterative extrapolation method for frequency bandlimited signal, can recover the entire signal from a part of it in the time domain [12,13]. As proven in [12], the received signal can gradually approximate the original signal, as the iterations tend to be infinite. Due to its high practicability and reliability, the GP algorithm has been adopted in many applications such as spectral estimation, high spectral efficiency communication and signal reconstruction [13–15]. When extrapolating the discrete signals, the influence of analyticity on the convergence of the GP algorithm should be considered. The feasibility and convergence of a discrete GP algorithm is provided and the effective sampling period is analyzed in [16,17]. The core computation uses either Fourier transform (FT) for analytic signals or discrete Fourier transform (DFT) for discrete signals, and a congruent relationship is established with continuous or discrete prolate spheroidal functions. To enlarge the application scope,

algorithms based on GP algorithm are extended to signals bandlimited into more domains such as the fractional Fourier domain, wavelet domain, or linear canonical transform domain [18–20]. Moreover, mathematic means-like regularization methods are further adopted to lower the extrapolation error led by white noise [21,22]. The acceleration of the extrapolation method is another research direction. A fast extrapolation method is proposed to improve the convergence of GP algorithm by sampling [23]. The direction of error reduction can also be improved by gradient descent or the core FT computation can be simplified to a Gram–Schmidt procedure in mathematic aspects [24].

The literatures regarding the GP algorithm were mostly focused on the generalized form or the implement-ability in some scenarios, but few about more efficient extrapolation. Two extrapolation problems of the GP algorithm have rarely been addressed in wireless communication scenarios. The one is the influence of Doppler frequency shift which causes the shift of center frequency and the bandwidth of the original signal. The influence on the extrapolation accuracy is obvious since the filter bandwidth during GP algorithm is always set equal to the bandwidth of original signal. To extrapolate a signal with frequency offset, the iteration filter with larger bandwidth is required to retain the shifted information beyond the original bandwidth, but the performance of iterative filter with large bandwidth have not been addressed. The other one is the duration of the received signal. The extrapolation efficiency when the known part is relatively short has not be discussed. Besides, some signals reveal better bandlimited characteristic in fractional Fourier domain, such as the optical code division multiplexing signal (OCDM) [25], which meets similar extrapolation problems to the frequency bandlimited signals. OCDM signals present similar subcarrier characteristics in the fractional Fourier domain to OFDM signals in the Fourier domain. The core computation of OCDM system is fractional Fourier transform (FrFT), which generalizes the linear differential process of FT [26]. From a physical perspective, time domain and frequency domain correspond to two orthogonal coordinate axes. FrFT rotates the orthogonal coordinate axis through a fractional variant, reflecting the time–frequency aggregation characteristics of signals [27]. Since the considerate aggregation of some non-frequency bandlimited signals such as the chirp signal in the fractional domain, FrFT is widely used in signal processing, radar, and wireless communications [27–30]. Research on the extrapolation of fractional bandlimited signal has already started. The iterative method in the time domain and the fractional domain is simulated and verified effective [20,29]. Whereas the extrapolating the process is limited by the truncation errors from the filter bandwidth. When the observed signal is relatively short, the efficiency of the iteration still degrades.

In this paper, we consider the problems of GP algorithm at two cases: (1) the observed signal is relatively short; and (2) frequency shift exists during transmission. A piecewise extrapolation method is proposed to solve the problems according to the error variation and error accumulation within the iterations of GP algorithm. The extrapolation process is divided into several pieces and the minimum energy least squares error extrapolation result based on GP algorithm is given to reduce the accumulated error. Problem 1 can be converted to the case that the compressed ratio is small. Problem 2 can be converted to the case that extrapolating signals with larger filter bandwidth. The piecewise extrapolation method is extended to FrFT domain to solve the problems of extrapolation for OCDM signals. The outline of this paper is organized as follows. In Section 2, some notations and properties of frequency bandlimited signals and fractional-domain bandlimited signals are addressed. The extrapolation process of GP algorithm is also introduced briefly in this section. In Section 3, the influence of the observed length of the known segment and the bandwidth of the filter used in GP algorithm on the extrapolation accuracy are analyzed, respectively. According to the problem formulation, a new piecewise extrapolation method is present in Section 4. Simulation results demonstrate the generality and the performance advantage of the proposed method against GP algorithm.

2. Problem Formulation

2.1. Bandlimited Signals

A typical σ -frequency bandlimited signals $f(t)$ should satisfy that $F(\omega) = 0$ for $\forall \omega \notin [-\sigma, \sigma]$, where σ is real and $F(\omega)$ is the Fourier transform result of $f(t)$.

As a generalized form of FT, p -order FrFT of a time domain signal $f(t)$ is defined as

$$F_p(u) = \mathcal{F}^p[f(t)](u) \equiv \int_{\mathbb{R}} K(p; t, u) f(t) dt, \tag{1}$$

where the kernel function $K(p; t, u)$ is represented as

$$K(p; t, u) = \begin{cases} \sqrt{\frac{1-j \cot \varphi}{2\pi}} e^{j \frac{t^2+u^2}{2} \cot \varphi - j \frac{tu}{\sin \varphi}}, & \varphi \neq n\pi \\ \delta(t - u), & \varphi = 2n\pi \\ \delta(t + u), & \varphi = (2n + 1)\pi \end{cases} \tag{2}$$

where $\varphi = p\pi/2$ is the rotation angle of the time-frequency plane, variant $p \in \mathbb{R}$ with the period of 4, and $n \in \mathbb{Z}$. When $p = 1$ and $\varphi = \pi/2$, (1) reduces to FT, and when $p = -1$ and $\varphi = -\pi/2$, (1) reduces to inverse FT (IFT). If $p = 0$, $F_0(u) = f(t)$.

In terms of a σ -fractional bandlimited signal $f(t)$, the values of its FrFT form should be zero outside the interval $[-\sigma, \sigma]$ as

$$F_p(u) = \mathcal{F}^p[f(t)](u) = 0 \text{ for } |u| \geq \sigma. \tag{3}$$

According to Parseval principle, the energy should be finite

$$\int_{\mathbb{R}} |f(t)|^2 dt = \int_{\mathbb{R}} |F_p(u)|^2 du < +\infty \tag{4}$$

where $\sigma > 0$ denotes the bandwidth of the original signal.

In the actual scenarios, some signals are not definitely bandlimited, but relatively. Take the OFDM signal as an example, the transmitted information is expected to be modulated into a series of orthogonal trigonometric basis functions. Due to the finite duration, energy dispersion exists in the actual OFDM signals, resulted in non-bandlimited characteristic (regardless of the lowpass filter processing). In that case, the OFDM signal can still be regarded as bandlimited since the dispersion is ignorable outside the original bandwidth. The compressed OFDM communication structure [9] is also proposed based on the relatively bandlimited characteristic.

2.2. Traditional GP Extrapolation Algorithm

GP extrapolation algorithm is proposed for analytic frequency bandlimited signals. To extrapolate an σ -bandlimited signal $f(t)$, the observed $g(t)$ is assumed to be

$$g(t) = f(t)\mathcal{U}_T(t) \tag{5}$$

where the operator $\mathcal{U}_T\{\}$ remains the part of $f(t)$ within $[-T, T]$ and T is positive.

The extrapolation is realized with iterations. For the first iteration $i = 1$, the initial signal is $f_0(t) = g(t)$. Defining $f_{i-1}(t)$ as the output result of $(i - 1)$ th iteration, and the i th iteration in GP algorithm consists of 6 main steps:

Input $f_{i-1}(t)$ as the initial signal of the i th iteration.

First, the signal $f_{i-1}(t)$ is transformed into the frequency domain with FT as $F_{i-1}(\omega)$.

Second, $F_{i-1}(\omega)$ is lowpass filtered within $|\omega| \leq \sigma$.

Third, the signal is transformed to the time domain with IFT.

Finally, the part within $[-T, T]$ is replaced by the observed part $g(t)$.

Output $f_i(t)$ as the result of the i th iteration.

2.3. Amplitude Variation during Extrapolation

The performance of the extrapolation method can be evaluated with mean-square error (MSE). In the case of $\Omega = \sigma$ for GP algorithm, the convergence can be explained with the relationship of $f(t)$, $f_{i-1}(t)$ and $f_i(t)$.

Define an MSE function as $\mathcal{M}\{f(t), g(t)\} = \int_{-\infty}^{\infty} |f(t) - g(t)|^2 dt$. Then it follows that $\mathcal{M}(f, f_{i-1}) > \mathcal{M}(f, g_i) > \mathcal{M}(f, f_i)$. The first greater-than relationship is attributed to that both f and g_i is bandlimited within $[-\Omega, \Omega]$, but f_i is not. The lowpass filter maintains the bandlimited characteristics of g_i in the 2nd step of GP algorithm in Section 2.2, thus the difference between f and f_i is larger than that of f and g_i . The second greater-than relationship is due to that the known signal within $t \in [-T, T]$ replaces the extrapolated part in the 4th step. The known part is obviously more accurate than the extrapolated one hence reducing the MSE.

According to GP algorithm referred in Section 2.2, the iteration filter in step 2 is set to be with the same bandwidth as that of the original signal. However, the actual signal to be extrapolated is finite in the time domain and it is not strictly bandlimited. Since the signal bandwidth may shift, and the bandwidth of iteration filter may be chosen larger. In addition, the maximum iteration is always set considering the computation requirement, which is not a fixed number. Therefore, the influence of the iteration filter and maximum iteration (stopping criterions) on MSE and amplitude variation should be discussed, respectively.

As for a basic isometric time domain signal $f(t) = \cos(2\pi t)$, the variation in the signal waveform shown in Figure 1 can reflect the extrapolation process more intuitively. The original cosine signal is sampled uniformly by 2048 points within $t \in (-4, 4)$, and the duration of signal to be extrapolated is determined by the truncated rate α . For example, duration of signal to be extrapolated is within $t \in (-1, 1)$ for $\alpha = 0.25$. Here the stopping criterions is set to be maximum iterations ITE, and the initial known signal $g(t) = f(t), |t| < 1$. The bandwidth of iteration filter is chosen to be the center frequency of f_1 in the condition of $\Omega = \sigma$. Two conditions are considered that are the waveforms under different maximum iterations (simplified as ITE in the simulation figures) and under different bandwidth values of iteration filter. The MSE of f and extrapolated $\hat{f} = f_{ITE}$ are shown in Figure 1, and waveforms of the extrapolated signal under different conditions are shown in Figure 2. The “ $r_{f/s}$ ” in the legend denotes the ratio of extrapolation filter bandwidth and signal bandwidth.

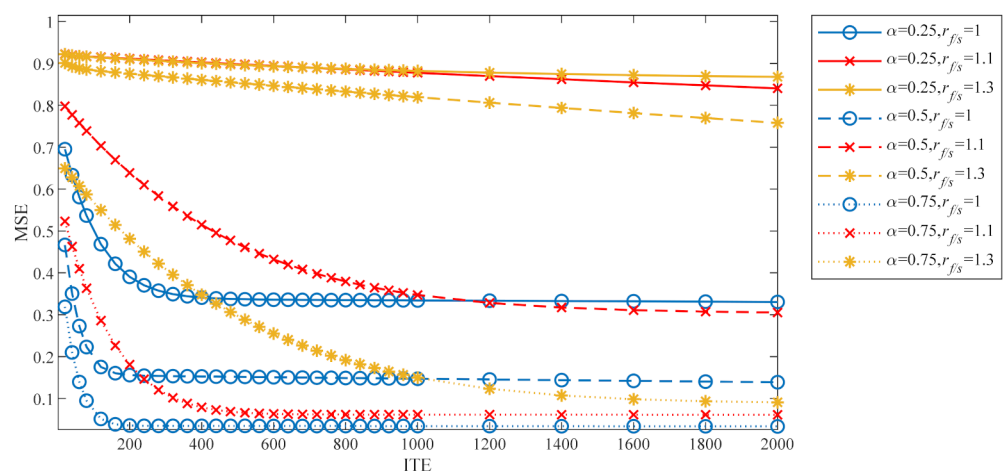
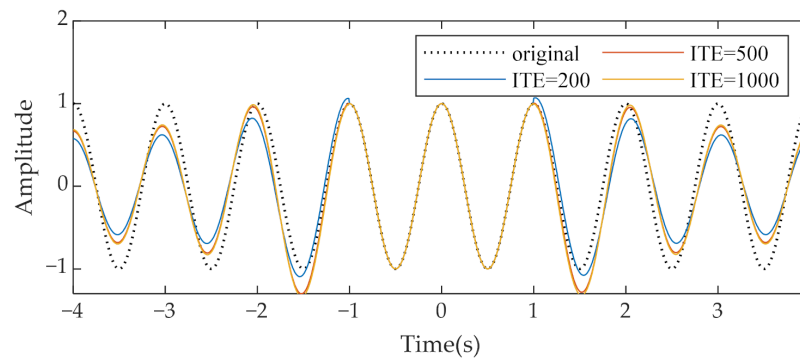
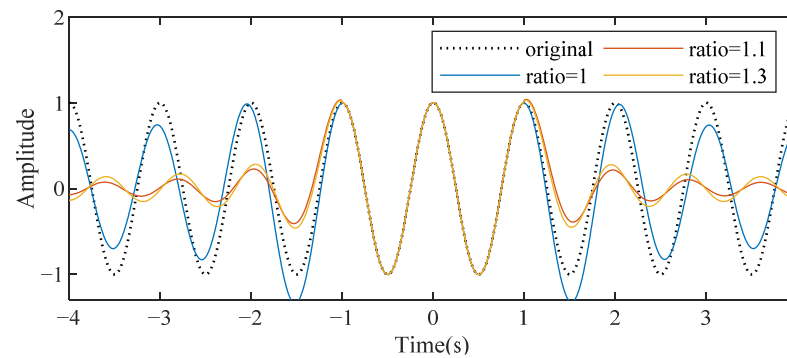


Figure 1. The MSE between f and g_{ITE} at different iteration filter bandwidth.



(a) The extrapolated waveform when $r_{f/s} = 1$ with different ITE.



(b) The extrapolated waveform when ITE = 1000 with different $r_{f/s}$.

Figure 2. The waveform comparison between original signal and extrapolated signals ($\alpha = 0.25$).

In Figure 1, all MSEs decrease with more iterations, reflecting a more accurate extrapolation. With the same $r_{f/s}$, the MSE is smaller when the truncated rate is larger. However, the MSE bottleneck appears during each extrapolation, especially when $r_{f/s} = 1$. For all truncated rate with $r_{f/s} = 1$, the bottleneck appears within 400 iterations and appears earlier with larger truncated rate. According to the theory of GP algorithm, it is attributed to the very small eigenvalue extrapolated with large iterations cannot improve the accuracy obviously though the whole extrapolation is convergent [18]. With the same truncated rate α , the best extrapolation presents with $r_{f/s} = 1$, and MSE performance deteriorates with larger ratio. Especially with small $\alpha = 0.25$, the MSEs at $r_{f/s} = 1.1$ and $r_{f/s} = 1.3$ turn larger by 120% compared with $r_{f/s} = 1$. Besides, the MSE improvement from $r_{f/s} = 1.3$ to $r_{f/s} = 1.1$ is slight, reflecting the extrapolation accuracy is difficult to improve by adjusting the extrapolation filter unless it is optimal ($r_{f/s} = 1$). Considering the influence of finite duration on the signal bandwidth, it can be inferred that the optimal ratio is not 1 for some other signals. In that case, an extrapolation convergence bottleneck should be solved and the extrapolation at large iteration filter bandwidth needs to be improved. For a fair comparison, the MSE reflects the difference at the extrapolated location and is normalized, defined as

$$\text{MSE}\{f(t), \hat{f}(t)\} = \frac{\int_{-\infty}^{\infty} |(1 - \mathcal{U}_T(t))(f(t) - \hat{f}(t))|^2 dt}{\int_{-\infty}^{\infty} |(1 - \mathcal{U}_T(t))f(t)|^2 dt} \quad (6)$$

In terms of the amplitude variation shown in Figure 2, the difference between the original signal and extrapolated signal reduces with more iterations. While in Figure 2a, the variation between ITE = 200 and 500 differs more than that between ITE = 500 and 1000, reflecting a gradually slower extrapolation convergence. Besides, the amplitude of the extrapolated part farther from the known part turns smaller and smaller. As for Figure 2b, the extrapolated waveform is closer the original one with less $r_{f/s}$ (where $r_{f/s} \geq 1$). The

bandwidth of the extrapolation filter causes obvious influences on the amplitude, leading huge reduction of the amplitude of extrapolated signal when $r_{f/s} > 1$ compared to that when $r_{f/s} = 1$. Moreover, when the location of extrapolated waveform is closer to the known part, the amplitude is closer to the original waveform.

From the above analysis and simulation results, it can be seen that the GP algorithm obtains a convergent error through infinite iterations but the iterations are restrained in the actual extrapolation process. Therefore, two main problems should be focused. One is the slow convergence (MSE bottleneck) when the ratio of proportion of the known part is small or the iterations reach some threshold. Another is the inaccurate extrapolation (low MSE) when the iteration filter bandwidth is bigger than the original bandwidth. Considering the gradually decreasing amplitude of extrapolated signal, a piecewise iterative extrapolation method could start from the part closer to the known part and then extend the extrapolated range. The description, simulation results, and analysis of this method would be discussed in the following sections.

3. Methods

3.1. Explanation of Piecewise Extrapolation Method

To explain the extrapolation process more clearly, we notate the known part and the part to be extrapolated, respectively. As for a frequency-domain bandlimited signal, it can be divided into two parts:

$$f(t) = \mathcal{U}_T\{f(t)\} + \mathcal{R}_T\{f(t)\} \tag{7}$$

The operator $\mathcal{R}_T\{\}$ remains the rest part. In addition, $\mathcal{B}_\Omega\{\}$ is an Ω -bandwidth lowpass filter operator denoted by

$$\mathcal{B}_\Omega\{f(t)\} = \int_{-\Omega}^{\Omega} F(\omega)e^{j\omega t} d\omega \tag{8}$$

(8) can also be expressed with convolution form as $\mathcal{B}_\Omega\{f(t)\} = f(t) * \frac{\sin(\Omega t)}{\pi t}$.

Assume the known part $g(t) = \mathcal{U}_T\{f(t)\}$, the fundamental extrapolation from $g(t)$ to get $f(t)$ can be expressed by

$$\begin{cases} f_i(t) = \mathcal{R}_T\{g_i(t)\} + g(t) \\ g_i(t) = \mathcal{B}_\Omega\{f_{i-1}(t)\} \end{cases} \tag{9}$$

where $i \in \mathbb{Z}^+$, $f_0 = g(t) = \mathcal{U}_T\{f(t)\}$. The output signal is $\hat{f}(t) = f_i(t)$ when meeting certain stopping criterion. Operating $\mathcal{B}_\Omega\{\}$ once will bring with one-time FT, one lowpass filtering, and another IFT. With the maximum iterations ITE and $(2N + 1)$ sample points in the extrapolation, the complexity from complex multiplication computation is with the order $\mathcal{O}(2 \cdot \text{ITE} \cdot (2N + 1) \log(2N + 1))$.

To M -piecewise extrapolate $f(t)$ from $g(t) = \mathcal{U}_T\{f(t)\}$, the part to be extrapolated is firstly divided into M pieces. If it is uniformly divided into the M pieces, the whole extrapolation process is decomposed into M sub-processes as shown in Figure 3.

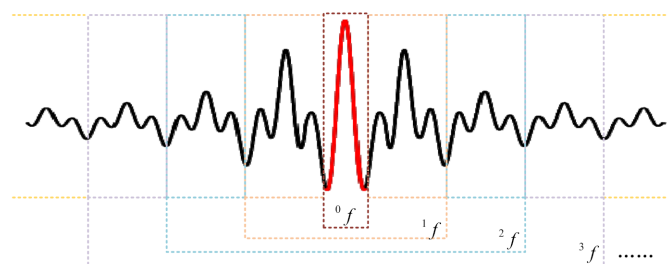


Figure 3. The relationship of pieces of piecewise extrapolation method.

In Figure 3, ${}^{m-1}f$ is the initial signal of the m th-piece extrapolation, and ${}^m f$ is supposed to be obtained at the end of the iteration at current piece. It can be found the iterations happen within the current piece, so is the error. The length of each piece is ΔT at both sides. The initial known part of each piece ${}^{m-1}f$ turns longer; if ${}^{m-1}f$ is extrapolated well enough, the accuracy of the m th-piece extrapolation would be improved. It is resulted from that less error accumulates within the shorter extrapolated part and the proportion of known signal increases. In practice, the signal to be extrapolated is a sampled received signal. The detailed piecewise extrapolation processes are explained as Table 1.

Table 1. M -piecewise extrapolation.

Iterative Steps of M -Piecewise Extrapolation
Initialization: $(-T, T)$ —the duration of $g(t)$, $(-T_0, T_0)$ —the duration of $f(t)$, M —the number of uniformly divided pieces of the extrapolated part, t_s —sampling period. On the positive side, the duration of each extrapolated piece is $\Delta T = (T_0 - T)/M$ with sampled points $\Delta N = \Delta T/t_s$. The original received signal is sampled to $g = \{g(n)\}$ where $ n \leq N$ and $N = T/t_s$.
Step 1: For the m th piece, the ${}^{m-1}f$ is zero-tapped on the extrapolated location to obtain the initial signal $\{{}^m f_0(n)\}$ where $ n \leq N_m$ and $N_m = N + m\Delta N$ points. When $m = 1$, ${}^0 f_0(n) = g(n)$ $ n \leq N$.
Step 2: For the i th iteration, the initial signal f_{i-1} is processed with DFT operator, lowpass filter and an IDFT operator to obtain g_i . When $i = 1$ $f_0(n) = {}^m f_0(n)$, $ n \leq N_m$.
Step 3: Replace the initial signal of $g_i(n)$ with ${}^m f(n)$ to obtain $f_i(n)$ as
$f_i = \mathcal{R}_{N_{m-1}}\{g_i\} + {}^m f_0 \tag{10}$
Step 4: (Judgement 1) If the iteration reaches the stopping criterion, continue to step 5; if not, update $i = i + 1$ and return to step 2.
Step 5: (Judgement 2) If $m = M$, output the extrapolation result as the extrapolation result $\hat{f}(n) = f_i(n)$; if not, update ${}^m f(n) = f_i(n)$, $m = m + 1$ and return to step 1.

In (10), the operator $\mathcal{R}_N\{\}$ remains the rest points beyond $(-N, N)$. The piecewise extrapolation degenerates into the discrete GP algorithm for $M = 1$.

The object of the above extrapolation method is the frequency domain bandlimited signal. Admittedly, the frequency bandlimited characteristic can be widely found in communication signals, but some signals show better energy accumulation characteristic in other domains. For instance, OCDM signals [25], with the orthogonal basis of chirp signals, is bandlimited in fractional Fourier domain.

As for a p -order FrFT bandlimited signal $f(t)$, a finite signal $g(t) = \mathcal{U}_T\{f(t)\}$ is observed. The piecewise extrapolation iteration could also be concluded with 4 steps, where the initial signal should transform to FrFT domain, then lowpass filtering, inversely transforming to time domain (IFrFT), and replacing by $g(t)$ within $[-T, T]$. A new formulation to describe the i th iteration of m th piece is shown as

$$\begin{cases} f_i(t) = \mathcal{R}_T\{\mathcal{B}_\Omega^p\{f_{i-1}(t)\}\} + g(t) \\ f_0(t) = g(t) \end{cases} \tag{11}$$

where $i \in \mathbb{Z}^+$. The operator $\mathcal{B}_\Omega^p\{\}$ denotes a σ -bandwidth lowpass filtering plus an inverse transform to the time domain, expressed as

$$\mathcal{B}_\Omega^p\{f(t)\} = \int_{-\Omega}^{\Omega} K(-p; t, u) F_p(u) du \tag{12}$$

where $F_p(u)$ is the p -order FrFT result of $f(t)$ as calculated in (1), and the kernel function $K(p; t, u)$ is presented in (2).

When $g(t)$ is sampled, the piecewise extrapolation follows the discrete procedure of (11)–(12). Similar to Table 1, the transform in step 2 should be DFrFT and IDFrFT accordingly. The implementation of the discrete transform can be found in [31].

3.2. The Minimum Energy Least Squares Error Solution of the Extrapolation

After sampled with the period t_s , the original signal f is a vector of $N_0 \times 1$ where $N_0 = T_0/t_s$ and g is a vector of $N \times 1$ where $N = T/t_s$. Define a truncator operator \mathcal{U} with the size of $N \times N_0$, the (n, u_n) elements is 1 where $n = 1, 2, \dots, N$ and the rest are zero. The known finite vector g can be expressed as $g = \mathcal{U}f$. If f is well frequency bandlimited, it follows that

$$f = \mathcal{B}f, \quad g = \mathcal{U}\mathcal{B}f \tag{13}$$

where \mathcal{B} represent a lowpass filter operator as $\mathcal{B}_\Omega\{\cdot\}$. The minimum energy least squares error extrapolation result \hat{f} follows that $\operatorname{argmin} \|g - \mathcal{U}\mathcal{B}\hat{f}\|^2$ [32]. As described in Table 1, the extrapolated result is 1f actually for the first sub-process starting from $\mathcal{U}_T\{f\}$ to $\mathcal{U}_{T+\Delta T}\{f\}$. The minimum energy least squares error extrapolation is considered as

$$\operatorname{argmin} \|g - \mathcal{U}\mathcal{B}[{}^1f]\|^2 \tag{14}$$

Since the discrete bandlimited signal f and the known part g can be expanded with discrete prolate spheroidal basis as [16], the result of (14) is expected to be ${}^1\hat{f} = \mathcal{B}\mathcal{U}^H\mathcal{B}_N^{-1}g$, where \mathcal{B}_N is a $(2N_1 + 1) \times (2N_1 + 1)$ matrix with the (v, u) element $\mathcal{B}_N(v, u) = \frac{\sin \Omega(v-u)}{\pi(v-u)}$.

However, the matrix \mathcal{B}_N will become ill conditioned and hard to compute the inverse matrix when N increases [31]. The iterative process shown in Table 1 cannot directly obtain the minimum energy least square error extrapolation result, but its error of each piece tends to zero when iterations tend to infinity.

3.3. Stopping Criterion and Complexity

The stopping criterion of an iterative extrapolation can be set according to the maximum iterations or MSE threshold, and can be modified with system requirements. It is noted that the accuracy of the former piece greatly affects the latter piece. Considering frequency shift will influence the bandwidth σ of original signal $f(t)$, the bandwidth of extrapolation filter is always set as $\Omega \geq \sigma$. As a result, $f(t) = \mathcal{B}_\Omega\{f(t)\}$ thus $g(t) = \mathcal{U}_T\{f(t)\} = \mathcal{U}_T\{\mathcal{B}_\Omega\{f(t)\}\}$.

Besides, the complexity of the extrapolation is restrained within a certain value in practice.

Suppose each piece iterates for ITE times, the complexity from complex multiplication computation is with the order $\mathcal{O}\left(2 \cdot \text{ITE} \cdot \sum_{m=1}^M (2N_m + 1) \log(2N_m + 1)\right)$. Thus, the multiple of the computational complexity when the number of pieces increases to M from 1 can be expressed as

$$\frac{\mathcal{O}\left(2 \cdot \text{ITE} \cdot \sum_{m=1}^M (2N_m + 1) \log(2N_m + 1)\right)}{\mathcal{O}(2 \cdot \text{ITE} \cdot (2N + 1) \log(2N + 1))} = \frac{\sum_{m=1}^M (2N_m + 1) \log(2N_m + 1)}{(2N + 1) \log(2N + 1)} \tag{15}$$

When the extrapolation samples are divided into M pieces uniformly, N_m increases uniformly from N_0 to N at the interval of $\Delta N = \frac{N-N_0}{M}$, hence obtaining $N_m = N_0 + m\Delta N$. More intuitively, the multiple of computation with different truncated rates α and pieces M according to (15) are listed in Table 2, respectively.

Table 2. Multiple of computation for M -piecewise extrapolation.

Values	$M = 2$	$M = 3$	$M = 4$	$M = 5$	$M = 6$
$\alpha = 0.25$	1.59	2.18	2.77	3.36	3.95
$\alpha = 0.50$	1.72	2.45	3.17	3.89	4.61
$\alpha = 0.75$	1.86	2.72	3.58	4.44	5.30

The multiple in Table 2 is the ratio between the computation of M -piecewise extrapolation and 1-piecewise extrapolation (GP algorithm) with the same maximum iterations for each piece. It can be seen that the multiple value is lower than the number of pieces M . The smaller truncated rates α is, the lower the multiple value is.

In addition to the stopping criterion of maximum iterations, MSE threshold can be also considered. The error of each piece will tend to zero when iterations tend to infinity whereas the infinite extrapolation cannot be implemented actually, which leads residual error for each piece. It should be admitted that dividing the extrapolated location into pieces will accumulate residual errors when the pieces ahead are not extrapolated to some accuracy. However, the error could be corrected when reaching some MSE threshold, which is attributed to the residual error is correlated to the known part g [13].

3.4. Bandwidth of Iteration Filter

It is noted that the length of the signal and the lowpass filter should be calculated for different pieces.

To extrapolate the m th piece, the initial signal has $(2N_{m-1} + 1)$ points and the result has $(2N_m + 1)$ points where $N_{m-1} = N + (m - 1)\Delta N$ and $N_m = N + m\Delta N$. Hence the initial signal is firstly zero-tapped to N_m points at both sides, which is equivalent to $N_m t_s$, and the frequency space between two points in the frequency domain should be $1/(N_m t_s)$. The length of the extrapolation filter with the bandwidth Ω should be corresponding to $N_\Omega = \lceil \Omega N_m t_s \rceil$ where $\lceil \cdot \rceil$ is a ceil operator.

Therefore, in the i th iteration of m th piece as shown in Table 1, the step 2 can also be expressed as

$$g_i = \mathbf{F}^{-1} \mathbf{H}_{N_\Omega} \mathbf{F} f_{i-1} \tag{16}$$

where the f_{i-1} is a vector of $(2N_m + 1) \times 1$; the lowpass matrix \mathbf{B} in (13) is equivalent to $\mathbf{F}^{-1} \mathbf{H}_{N_\Omega} \mathbf{F}$; \mathbf{F} and \mathbf{F}^{-1} are DFT matrix of $(2N_m + 1) \times (2N_m + 1)$ and its inverse matrix (IDFT matrix), respectively; and \mathbf{H}_{N_Ω} denotes a lowpass filter matrix for spectral sample as

$$\mathbf{H}_{N_\Omega} = \begin{bmatrix} \mathbf{I}_{N_\Omega+1} & \cdots & \mathbf{0} \\ \vdots & \mathbf{0} & \vdots \\ \mathbf{0} & \cdots & \mathbf{I}_{N_\Omega} \end{bmatrix}_{(2N_m+1) \times (2N_m+1)} \tag{17}$$

Since the known part can be considered as $g = Uf$, equivalent to a convolution in the frequency domain. The spectral leakage caused by convolution with discrete sinc signal will lead that the discrete bandwidth of original signal is longer than $N_\sigma = \lceil \sigma N_m t_s \rceil$. Moreover, the iteration filter bandwidth should consider the periodicity of the known part and the original signal.

4. Results and Discussion

Numerical examples are used to illustrate the performance of piecewise extrapolation method when the bandwidth of iteration filter is larger than σ and the truncated rate α is small. The original signals are selected from typical signal forms in communication field. Table 3 lists the explanation and the value of variables regarding GP algorithm or proposed method in the simulation.

Table 3. Variables Explanation.

Variable	Explanation	Value
α	Truncated rate.	0.25, 0.50
N	The number of sampled points of original signal.	1024
N_0	The number of points of truncated signal from original signal.	N_0
N_m	The number of points of the aim signal in m th piece extrapolation.	N_m
M	The number of pieces for piecewise extrapolation method.	1~6
$r_{f/s}$	The ratio between the bandwidth of iteration filter and original signal	1.0~1.5
ITE	The maximum iterations of each piece for piecewise extrapolation method.	0~4000

Noted that the comparison of performance should be conducted under the same computational complexity for fairness. The relationship of the traditional GP algorithm and M -piecewise extrapolation method can be found in Table 2. For instance, the MSE value of GP at ITE = 1000 when $\alpha = 0.25$ should be compared to that of 2-piecewise extrapolation method at ITE = 1000/1.59, 3-piecewise extrapolation method at ITE = 1000/2.18, and the rest can be carried out in the same manner.

A typical frequency bandlimited signal $f(t) = \sin c(t)$, $|t| \leq 4$ is sampled for $N = 1024$ points. Figure 3 compares MSEs of different $r_{f/s} = 1$ and different M at truncated rate $\alpha = 0.25$, calculated by (6). The decreasing MSE with gradually slowing rate reflects the convergence of the extrapolation method in Figure 4.

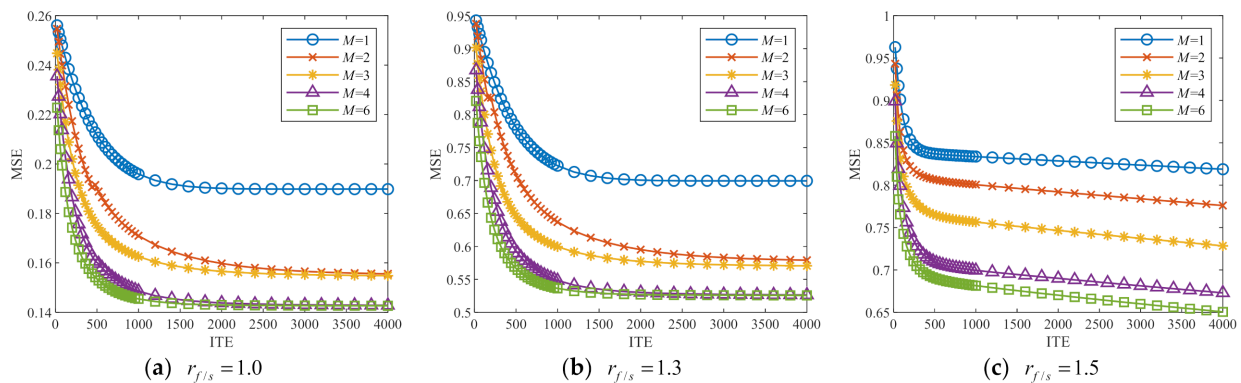


Figure 4. MSE of M -piecewise extrapolation for the signal $f = \sin c(t)$, $(-4 < t < 4)$ at $\alpha = 0.25$.

At $M = 1$ and ITE = 1000, the MSE reaches 0.19 at $r_{f/s} = 1$, 0.71 at $r_{f/s} = 1.3$ and 0.83 at $r_{f/s} = 1.5$, and then the variation of MSE becomes mild. For a fair comparison, the MSE should be discussed under the same level of computation. Combined with the multiple values in Table 2, the computation increases to 2–4 times when M increases from 2 to 6 with $\alpha = 0.25$. When the computation is fixed at ITE = 1000 ($M = 1$), the computation is close to those of ITE = 600 at $M = 2$, ITE = 500 at $M = 3$, ITE = 400 at $M = 4$ and ITE = 250 at $M = 6$. As for Figure 4a, the descending order of MSEs for different M is $(M = 1) \approx (M = 2) > (M = 3) > (M = 4) \approx (M = 6)$. When ITE increases to 4000, MSEs of different M -piece extrapolation varies relatively mildly, but in different levels. Compared to $M = 1$, the MSE at $M = 2, 3, 4, 6$ decreases by 19.7%, 18.4%, 24.2%, and 25.8%, respectively. It reflects that piecewise extrapolation can improve the extrapolation accuracy of original GP algorithm at the same computation but that too many pieces may not lead further performance improvements.

In the cases of larger bandwidth of iteration filter as shown in Figure 4b,c, the accuracy of extrapolation turns worse but the improvements from M -piecewise method differ more apparently. Suppose the maximum frequency shift is 50%, it is reasonable to set the bandwidth of the iteration filter to 1.5 times. At $r_{f/s} = 1.5$, the MSE at $M = 2, 3, 4, 6$ decreases by 5.3%, 11.1%, 17.8%, and 20.6%, respectively, compared to $M = 1$. Besides, the mild variation exists at different ITEs which are 2000 for $r_{f/s} = 1$, 3000 for $r_{f/s} = 1.3$ and

more than 4000 for $r_{f/s} = 1.5$. It illustrates that the M -piece extrapolation enables the MSE to descend longer and improve the accuracy of original GP algorithm.

Cosine signals, sine signals and their sum are common signal forms in wireless communication field. They are all periodic, which is different from the sinc signals above. In the compressive OFDM transmission system, the original OFDM signal can be truncated up to 0.5 to ignore the influence of self-interference on BER [15]. Therefore, the truncated rate α of those signals are chosen as 0.5 to simulate the MSE performance of piecewise extrapolation for compressed OFDM signals in Figure 5.

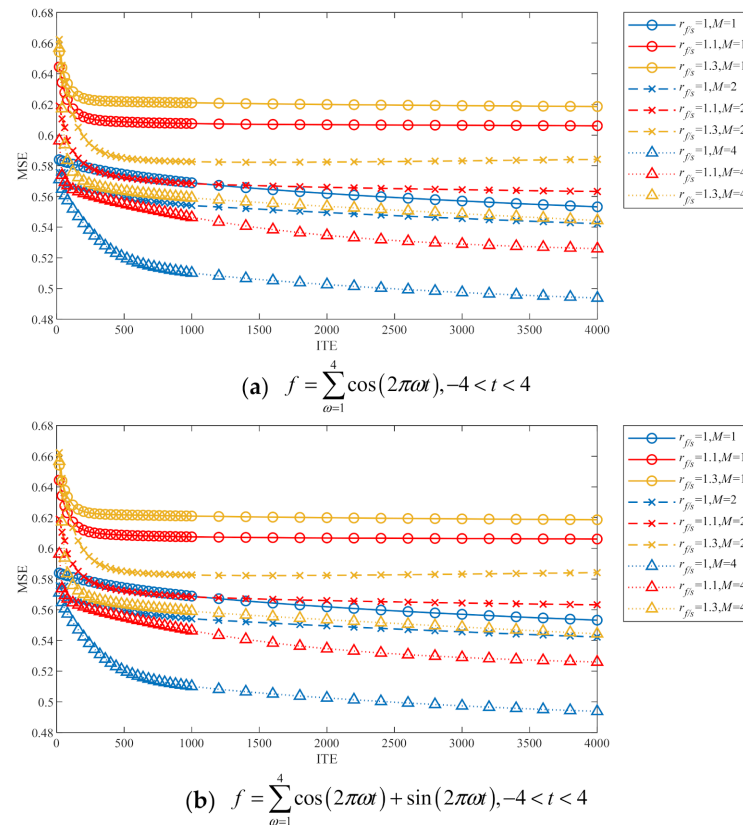


Figure 5. MSE of piecewise extrapolation for cosine and sine signals at $\alpha = 0.5$.

The sum of cosine signals and cosine/sine signals belong to one-way mapping compressed OFDM signals and two-way mapping compressed OFDM signals [8], respectively, in Figure 5a,b. The original signal f is sampled for $N = 1024$ points. Note that the $r_{f/s}$ 1.1 and 1.3 represents that the maximum carrier frequency offset is 0.1 and 0.3 respectively, which is a little different from the explanation in Table 3.

The improvements of piecewise extrapolation for compressed OFDM signal on MSE is can be found in Figure 5, especially when the bandwidth of iteration filter is larger than the original bandwidth. For piecewise extrapolation with larger M , the mild-variation area of MSE appears later with lower MSE at the same $r_{f/s}$ and computational complexity. From Figure 5a,b, more complex mapping form leads higher MSE but not double at the same $r_{f/s}$ and M . Similarly, in Figure 4b, the MSE at ‘ratio = 1.1, $M = 4$ ’ is lower than that at ‘ratio = 1, $M = 1$ ’, and so it is at ‘ratio = 1.3, $M = 4$ ’. It can be seen that the truncation error caused by large iteration filter bandwidth can be suppressed by piecewise method.

To verify the feasibility of the proposed method for FrFT bandlimited signal, an LFM signal $f = \exp(j2\pi\omega_0 t + j\pi k t^2)$ is selected since energy concentration characteristics of its FrFT spectrum at the fraction angle $\varphi = -\text{arccot}k$. The original signal is with $\omega_0 = 8$, $k = 1$, $|t| < 4$ and is sampled for $N = 1024$ points. Considering that the discrete FrFT spectrum of LFM signal is enveloped in sinc shape, the original signal bandwidth is selected as its first zero-crossing point which is a little larger than the computational result from φ . Combined

with the preliminary of FrFT and the piecewise extrapolation method, the MSEs at different $r_{f/s}$ and M 's are illustrated in Figure 6.

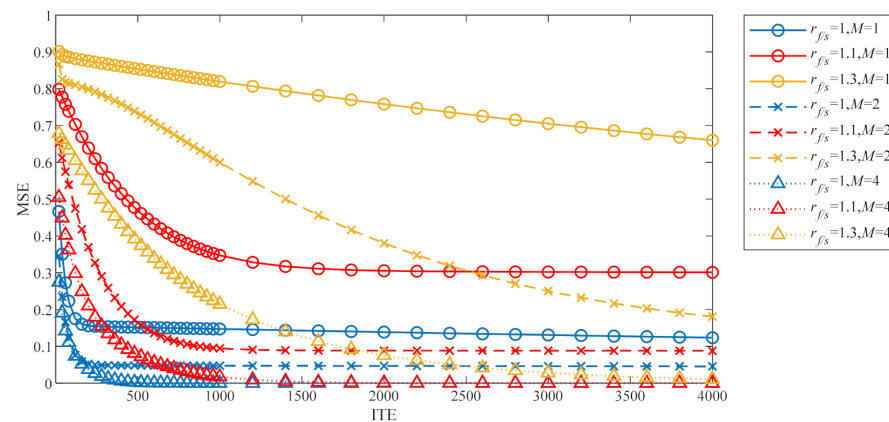


Figure 6. MSE of piecewise extrapolation for OCDM signal.

As shown in Figure 6, the piecewise extrapolation method enables to improve the accuracy of GP based extrapolation method ($M = 1$) for the OCDM signal, and the improvement is more obvious with larger $r_{f/s}$. When comparing the MSE at the same $r_{f/s}$ but different M , the mild-variation area at different M appears at similar ITE but with different computational complexity and MSE values. For instance, the mild-variation area of MSE appears at ITE = 1000 for all M 's at $r_{f/s} = 1.1$, but the total iterations are different. Referred to Table 2, the total computation of $M = 2$ and $M = 4$ are 1.72 times and 3.17 times than that of $M = 1$, respectively. With a fixed computational complexity of ITE = 4000 and $M = 1.0$, the MSEs of 2-piece extrapolation and 4-piece extrapolation decrease by 60% and another 95% at $r_{f/s} = 1$, 60% and another 88% at $r_{f/s} = 1.1$, and 52% and another 46% at $r_{f/s} = 1.3$. From the perspective of improvement degree, the proposed method behaves better at the $r_{f/s}$ closer to 1.

5. Conclusions

In this correspondence, an M -piecewise extrapolation method is proposed to improve the accuracy of a GP algorithm at the same computational complexity. The proposed method involves the extrapolation for Fourier domain and fractional Fourier domain bandlimited signals, of which the classical GP algorithm is a special case. Simulation results show the MSE superiority of the proposed method compared with GP algorithm or GP-based extrapolation algorithm for frequency bandlimited signals and FrFT bandlimited signals, respectively. The improvement from proposed method with 2~4 pieces is obvious in general with different bandwidth of iteration filter and truncated rates. When the GP algorithm reaches the MSE bottleneck, the MSE of proposed method is basically more than 5% lower than GP and can be improved further. When the proposed method reaches the MSE bottleneck, the MSE is more than 20% lower than GP at the same computational complexity. Moreover, the influence of the factors including number of pieces, the bandwidth of iteration filter and truncated rate on MSE and computational complexity is analyzed and quantified. When the iteration filter bandwidth is larger or the truncated rate is relatively small, the extrapolation accuracy can be lifted through increasing M under the same computational complexity (but too many pieces may not lead further performance improvement).

Author Contributions: Conceptualization, Y.Z. and X.S.; methodology, Y.Z.; writing—original draft preparation, Y.Z.; writing—review and editing, Y.Z., X.F., X.S. and X.L. All authors have read and agreed to the published version of the manuscript.

Funding: This research was funded by National Natural Science Foundation of China under Grant 62171151, by Natural Science Foundation of Heilongjiang Province of China under Grant YQ2021F003; by the National Natural Science Foundation of China under Grant 61901140 and by Science and Technology on Communication Networks Laboratory under Grant SCX21641X003.

Institutional Review Board Statement: Not applicable.

Informed Consent Statement: Not applicable.

Data Availability Statement: Not applicable.

Acknowledgments: The authors would like to acknowledge all the participants for their contributions to this research study.

Conflicts of Interest: The authors declare no conflict of interest.

References

1. Biondi, F. Recovery of Partially Corrupted SAR Images by Super-Resolution Based on Spectrum Extrapolation. *IEEE Geosci. Remote Sens. Lett.* **2016**, *14*, 139–143. [[CrossRef](#)]
2. Adam, K.; Scholefield, A.; Vetterli, M. Sampling and Reconstruction of Bandlimited Signals With Multi-Channel Time Encoding. *IEEE Trans. Signal Process* **2020**, *68*, 1105–1119. [[CrossRef](#)]
3. Hasar, U.C.; Ozturk, H.; Korkmaz, H.; Izginli, M.; Karaaslan, M. Improved line–line method for propagation constant measurement of reflection-asymmetric networks. *Measurement* **2022**, *192*, 110848. [[CrossRef](#)]
4. Hui, Y.; Su, Z.; Luan, T.H.; Li, C. Reservation Service: Trusted Relay Selection for Edge Computing Services in Vehicular Networks. *IEEE J. Sel. Areas Commun.* **2020**, *38*, 2734–2746. [[CrossRef](#)]
5. Yin, Z.; Jia, M.; Cheng, N.; Wang, W.; Lyu, F.; Guo, Q.; Shen, X. UAV-Assisted Physical Layer Security in Multi-Beam Satellite-Enabled Vehicle Communications. *IEEE Trans. Intell. Transp. Syst.* **2021**, *23*, 2739–2751. [[CrossRef](#)]
6. Amirhossein, N.; Mohammad, B.; Abdolali, A.; Muharrem, K. A reflection-only method for characterizing PEC-backed anisotropic materials using waveguide higher order modes. *Int. J. RF Microw. Comput.-Aided Eng.* **2020**, *30*, e22340.
7. Hui, Y.; Cheng, N.; Su, Z.; Huang, Y.; Zhao, P.; Luan, T.H.; Li, C. Secure and Personalized Edge Computing Services in 6G Heterogeneous Vehicular Networks. *IEEE Internet Things J.* **2021**, *accepted*. [[CrossRef](#)]
8. Jia, M.; Yin, Z.; Li, D.; Guo, Q.; Gu, X. Toward Improved Offloading Efficiency of Data Transmission in the IoT-Cloud by Leveraging Secure Truncating OFDM. *IEEE Internet Things J.* **2019**, *6*, 4252–4261. [[CrossRef](#)]
9. Zhang, Y.; Li, Y.; Fang, X.; Sha, X.; Feng, Y.; Wang, W. Towards Spectral Efficiency Enhancement for IoT Aided Smart Transportation: A Compressive OFDM Transmission and Regularized Recovery Approach. *EURASIP J. Adv. Signal Process* **2021**, *in press*. [[CrossRef](#)]
10. Prasad, K.N.R.S.V.; Hossain, E.; Bhargava, V.K. Machine Learning Methods for RSS-Based User Positioning in Distributed Massive MIMO. *IEEE Trans. Wirel. Commun.* **2018**, *17*, 8402–8417. [[CrossRef](#)]
11. Hui, Y.; Su, Z.; Luan, T.H. Unmanned Era: A Service Response Framework in Smart City. *IEEE Trans. Intell. Transp. Syst.* **2021**, *in press*. [[CrossRef](#)]
12. Papoulis, A. A new algorithm in spectral analysis and band-limited extrapolation. *IEEE Trans. Circuits Syst.* **1975**, *22*, 735–742. [[CrossRef](#)]
13. Gerchberg, R. Super-resolution through Error Energy Reduction. *Opt. Acta Int. J. Opt.* **1974**, *21*, 709–720. [[CrossRef](#)]
14. Jain, A.; Ranganath, S. Extrapolation algorithms for discrete signals with application in spectral estimation. *IEEE Trans. Acoust. Speech Signal Process* **1981**, *29*, 830–845. [[CrossRef](#)]
15. Ozan, W.; Jamieson, K.; Darwazeh, I. Truncating and oversampling OFDM signals in white Gaussian noise channels. In Proceedings of the 2016 10th International Symposium on Communication Systems, Networks and Digital Signal Processing (CSNDSP), Prague, Czech Republic, 20–22 July 2016; pp. 1–6. [[CrossRef](#)]
16. Sanz, J.; Huang, T. Some aspects of band-limited signal extrapolation: Models, discrete approximations, and noise. *IEEE Trans. Acoust. Speech Signal Process* **1983**, *31*, 1492–1501. [[CrossRef](#)]
17. Schlebusch, H.; Splettstosser, W. On a conjecture of J.L.C. Sanz and T.S. Huang. *IEEE Trans. Audio Speech Lang. Process* **1985**, *33*, 1628–1630. [[CrossRef](#)]
18. Kauppinen, I.; Roth, K. Improved noise reduction in audio signals using spectral resolution enhancement with time-domain signal extrapolation. *IEEE Trans. Speech Audio Process* **2005**, *13*, 1210–1216. [[CrossRef](#)]
19. Farsiu, S.; Robinson, M.D.; Elad, M.; Milanfar, P. Fast and Robust Multiframe Super Resolution. *IEEE Trans. Image Process* **2004**, *13*, 1327–1344. [[CrossRef](#)]
20. Shi, J.; Sha, X.; Zhang, Q.; Zhang, N. Extrapolation of Bandlimited Signals in Linear Canonical Transform Domain. *IEEE Trans. Signal Process* **2011**, *60*, 1502–1508. [[CrossRef](#)]
21. Chen, M.; Qu, G.; Shi, L.; Gao, S. The reweighted Landweber scheme for the extrapolation of band-limited signals. *Signal Process* **2019**, *164*, 340–344. [[CrossRef](#)]
22. Xu, S.; Tao, S.; Chai, Y.; Yang, X.; He, Y. The extrapolation of bandlimited signals in the offset linear canonical transform domain. *Optik* **2018**, *180*, 626–634. [[CrossRef](#)]

23. Chen, W. A Fast Convergence Algorithm for Band-Limited Extrapolation by Sampling. *IEEE Trans. Signal Process* **2008**, *57*, 161–167. [[CrossRef](#)]
24. Salomon, B.; Ur, H. Accelerated Iterative Band-Limited Extrapolation Algorithms. *IEEE Signal Process Lett.* **2004**, *11*, 871–874. [[CrossRef](#)]
25. Omar, M.S.; Ma, X. Performance Analysis of OCDM for Wireless Communications. *IEEE Trans. Wirel. Commun.* **2021**, *20*, 4032–4043. [[CrossRef](#)]
26. Namias, V. The Fractional Order Fourier Transform and its Application to Quantum Mechanics. *IMA J. Appl. Math.* **1980**, *25*, 241–265. [[CrossRef](#)]
27. Liu, X.; Shi, J.; Sha, X.; Zhang, N. A general framework for sampling and reconstruction in function spaces associated with fractional Fourier transform. *Signal Process* **2015**, *107*, 319–326. [[CrossRef](#)]
28. Martone, M. A multicarrier system based on the fractional Fourier transform for time-frequency-selective channels. *IEEE Trans. Commun.* **2001**, *49*, 1011–1020. [[CrossRef](#)]
29. Sharma, K.K.; Joshi, S.D. Extrapolation of signals using the method of alternating projections in fractional Fourier domains. *Signal Image Video Process* **2007**, *2*, 177–182. [[CrossRef](#)]
30. Zou, L.; Sato, M. An Efficient and Accurate GB-SAR Imaging Algorithm Based on the Fractional Fourier Transform. *IEEE Trans. Geosci. Remote Sens.* **2019**, *57*, 9081–9089. [[CrossRef](#)]
31. Candan, C.; Kutay, M.A.; Ozaktas, H.M. The Discrete Fractional Fourier Transform. *IEEE Trans. Signal Process* **2000**, *48*, 1329–1337. [[CrossRef](#)]
32. Zhao, H.; Wang, R.; Song, D.; Zhang, T.; Wu, D. Extrapolation of discrete bandlimited signals in linear canonical transform domain. *Signal Process* **2014**, *94*, 212–218. [[CrossRef](#)]